COST EFFECTIVE GROWTH OF SILICON MONO INGOTS BY THE APPLICATION OF THE MULTIPULLING TECHNIQUE COMBINED WITH ACTIVE CRYSTAL COOLING

F. Mosel[1], A.V. Denisov[1], B. Klipp[1], N. Sennova[1], M. Herms[2], R. Kunert[3], P. Dold[3]
[1] PVA Crystal Growing Systems GmbH, Im Westpark 10-12, 35435 Wettenberg, Germany
[2]PVA Metrology & Plasma Solutions GmbH, Am Naßtal 6/8, 07751 Jena-Maua, Germany
[3] Fraunhofer CSP, Otto-Eissfeldt-Str. 12, 06120 Halle/Saale, Germany
frank.mosel@pvatepla.com, phone: +49 64168690-125, fax: +49 64168690-822

ABSTRACT: The permanent demand for the improvement of solar cell efficiency and reduction of production costs has placed much focus on the multiple Cz-pulling techniques from a single crucible. PVA Crystal Growing Systems GmbH has developed a mobile recharge system for Czochralski pullers, the SiCharger MRS. This system can operate several Cz-pullers with in a consecutive mode and is characterized by low investment costs, reduced silicon consumption and higher output per crucible. This system and its potential were presented in detail at the 33rd EU PVSEC [1]. Another way to save costs due to an increased productivity is a higher pull rate. In order to enable a higher pull speed under stable crystal growth conditions, the hot zone was investigated and optimized by simulating the entire crystal growth arrangement with the commercial program package CGSim [2]. As a result, the pull rate could be increased significantly. In a next approach, an active crystal cooling system was implemented. This cooling device itself consists of a water cooled container, which is placed above the phase boundary of the growing crystal, in order to increase the axial temperature gradient in the growing crystal close to its solidification interface. This system is described in detail in [3]. With this arrangement the heat transport through the crystal is improved so that crystals with 8 inch diameter were grown with a pull rate of 1.8 mm/min resulting in an appreciable saving of process costs.
Keywords: c-Si, multipulling, active crystal cooling, melt replenishment, growth rate

1 INTRODUCTION

About 90% of the solar cells produced in the world are based on crystalline silicon (c-Si). The wafer market is already dominated by monocrystalline Si-material and the trend of increasing market share will continue as shown in fig.1. It is expected that in the next 10 years the market share of mono-Si will surpass the 60% mark. This market development is driven by the increasing demand for high-performance cells, but in presence of further increasing cost pressure. The cost reduction cannot be achieved by the wafer manufacturers only by reducing the consumption costs. A drastic increase in productivity while increasing product performance is essential.

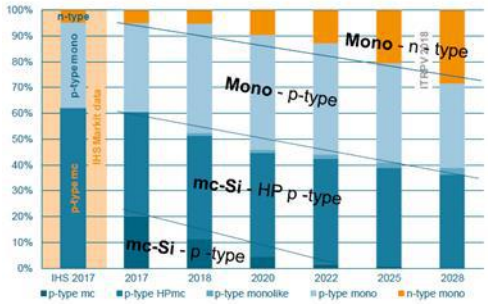

Figure 1: World market shares for wafer / ingot types. (International Technology Roadmap for Photovoltaic Results 2017 – Presentation)

Since the existing Czochralski pullers for the PV industry are limited regarding the melt volumes (crucible sizes) or the resulting crystal lengths, the pulling of several crystals from a single crucible (multipulling) is a necessary consequence. To increase productivity, maximizing the pull rate is the most powerful tool in the Cz-process. By a combination of both methods a maximum effect concerning cost savings can be achieved. In the following sections we describe the equipment for these low cost process conditions. The material properties of the crystals grown with this equipment are presented, an economic consideration of this process technique is given.

2 EXPERIMENTAL

2.1 Crystal growth equipment

The crystal growth experiments presented in this paper were performed in a SC24/26 Czochralski-puller from PVA Crystal Growing Systems GmbH. The crystal growth experiments were performed in a 24 inch hot zone. For larger melt volumes of up to 300 kg, a 26 inch hot zone will be available soon for this puller type.

2.2 Hotzone design with and without active crystal cooling

The physical limiting parameter for the growth rate of ingots in a Czochralski configuration is the dissipation of the latent heat of fusion of silicon at the interface crystal/melt by heat conduction through the growing crystal. The heat received by the ingot in contact with its melt can be determined as the heat of solidification plus the heat flux from the melt into the ingot. This situation can be written in a simple one dimensional model:

$$\lambda_s \cdot A \cdot \left(\frac{dT}{dx}\right)_S = \lambda_l \cdot A \cdot \left(\frac{dT}{dx}\right)_l + \rho \cdot A \cdot L \cdot v_p \quad (1)$$

in which λ is the thermal conductivity, A is the cross section of the ingot, (dT/dx) is the axial temperature gradient, v_p is the constant growth velocity, ρ is the crystal density, L is the latent heat of fusion and s,l are the subscripts for the solid and liquid phase. Assuming an isothermal melt i.e. $(dT/dx)_l = 0$ the maximum pull rate v_{pmax} can be estimated and related to the crystal radius r:

$$(2) \quad \lambda_s \cdot \mathrm{A} \cdot \left(\frac{dT}{dx}\right)_S = \lambda_l \cdot \mathrm{A} \cdot \left(\frac{dT}{dx}\right)_l + \rho \cdot \mathrm{A} \cdot L \cdot v_p$$

Here σ is the Stefan-Boltzmannn constant, ε is the surface emissivity, m is the subscript for melting temperature. For a detailed derivation of the equations (1) and (2) see E. Billig [4].

To come closer to the theoretical limit of the maximum pull speed v_{pmax} the SC24-puller was equipped with an active crystal cooling (acc) system. Fig.2 shows a sketch of the active crystal cooling system which consists of a water cooled container in form of a coil which is placed between the inner heatshield and the growing crystal. The purpose of the cooling device is to alter the axial temperature gradient at the crystallization front in the crystal. The main influencing parameters of the cooling element are the cooling power given by the geometry and the cooling water flow, the vertical distance to the melt surface, the radial distance to the crystal and the emissivity of the cooling element. The crystal growth configuration including the active cooling system was developed and optimized by means of numerical simulation. calculations using the CGSim-

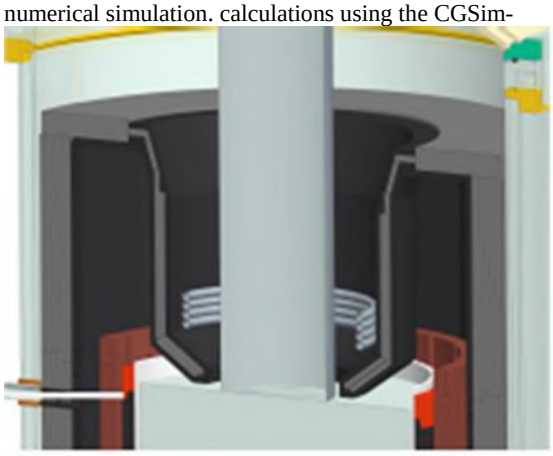

Figure 2: Arrangement of the active crystal cooling device in the hotzone

software-package from STR [2]. The most important evaluation criteria of the hotzone are the deflection of the phase boundary (concavity) and the radial temperature distribution on the melt surface. The phase boundary should be as plane as possible and the radial temperature gradient at the triple point for stable growth conditions should be steep. Fig.3 shows the interface curvature H of the phase boundary versus the average pull speed in the body phase at a body length of 500 mm for the different crystal growth configurations examined in this project (for details see [3]). Three different regions are shown in the diagram. In the stable growth region (green) the system is insensitive to changes in the average pull speed. This region is robust and suitable for industrial production. In the metastable growth region (yellow) all growth parameters have to be well tuned. Small changes can lead to unstable growth with loss of shape, i.e. spiral growth. In the unstable growth region (red) no regular crystal growth is possible. In the graph the points connected by the lines represent individual results of the simulation calculations for the examined crystal growth arrangements (V1-V5). The red circles in the graph represent experimental results. The configuration V1 is a standard configuration with a pull speed of 0.9 mm/min in the body phase. In the optimized configuration V2 an average pull speed of 1.3 mm / min could be established without an active crystal cooling. The configuration V5 with active crystal cooling shows the best values in terms of pull speed and energy saving by the optimized hot zone configuration (see tab.3). Configurations V3 and V4 were intermediate steps and will not be considered further.

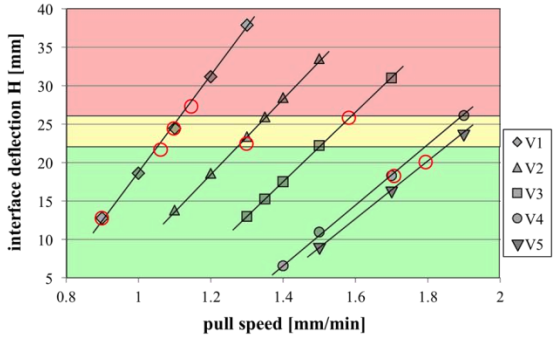

Figure 3: State diagram of the stable (green), metastable (yellow) and unstable (red) growth conditions for the different hotzone configurations. The main parameter: deflection H of the interface shape is plotted versus the pull speed and shown in fig.4.

Fig. 5 shows the dependence of the phase boundary deflection from the distance of the inner heat shield to the melt surface for different pulling rates in the growth configuration V5. In addition to the deflection of the phase boundary, the radial temperature distribution is an essential parameter for stable growth conditions. The radial temperature distribution on the melt surface depends on the cooling element in connection with the growth rate. As the pull rate increases, more heat of crystallization is released which reduces the radial temperature gradient and the formation of a supercooled area near the solidification front may occur, interfering with stable growth of the constant diameter crystal [5]. The dependence of the radial temperature distribution on the pull rate on the one hand and on the distance between the inner heat shield and the melt surface on the other hand is shown in figs.6 and 7. Together with the phase boundary deflection, these parameters must be reconciled to achieve optimal growth conditions.

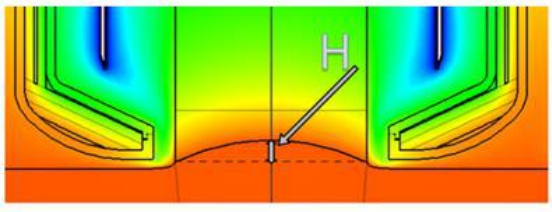

Figure 4: Sketch of the cooling device and the inner heat shield. H indicates the deflection of the phase boundary.

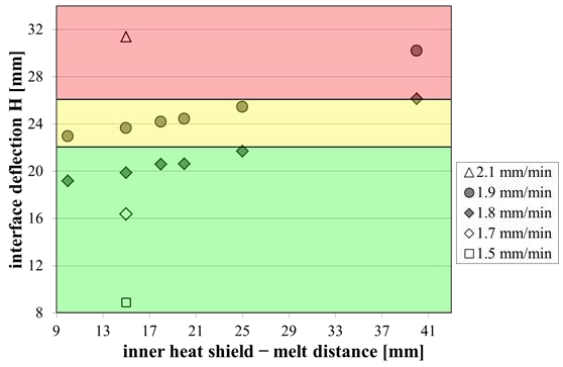

Figure 5: State diagram of the stable (green), metastable (yellow) and unstable (red) growth conditions for different distances of the inner heat shield to the melt surface in crystal growth configuration V5. The symbols represent results of numerical calculations.

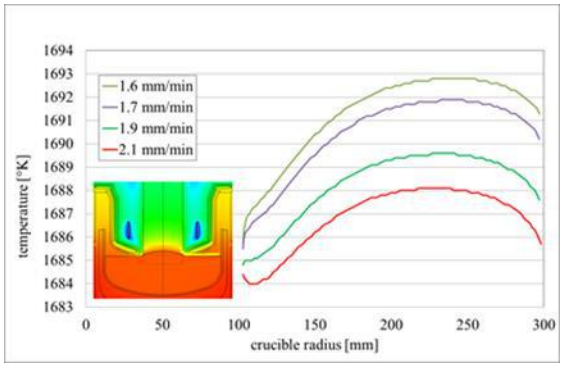

Figure 6: Radial temperature distributions (yellow marker in the inserted picture) on the melt surface for different growth rates in crystal growth configuration V5

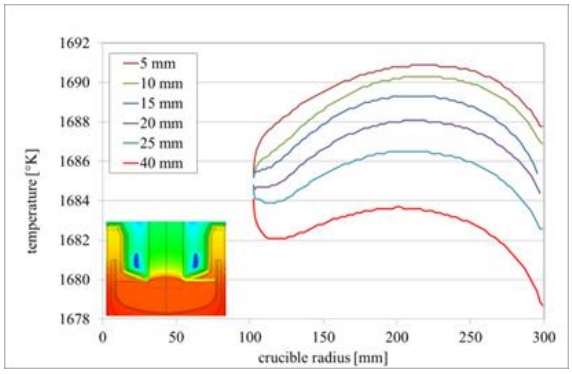

Figure 7: Radial temperature distributions (yellow marker in the inserted picture) on the melt surface for different distances between the melt surface and the inner heat shield in crystal growth configuration V5

The hotzone and crystal growth parameters used in this work were also evaluated for the calculated stresses in the crystals. Assuming isotropic material properties, the von Mises-stresses can be estimated. The von-Mises-stress is a theoretical value expressing a three-dimensional stress state as a scalar. The von-Mises-stress is therefore a viable criterion for judging crystal growth conditions with regard to the probability of dislocation formation [6]. A value of 80 MPa is considered as a critical value for the growth conditions of 8-inch silicon crystals [7]. The results, summarized in tab.2 later in this report, are all well below the critical value.

2.3 Mobile Recharge System

In the standard Cz batch process, one single crystal is pulled out of a single crucible. After this process is finished and the system is cooled down, the next process is prepared. This type of process management is very time-consuming and cost-intensive. In each process, one crucible is consumed and the hotzone is heavily stressed by the temperature cycles. In order to extend hotzone lifetime and to reduce crucible consumption, the multipulling process has been established, in which several crystals are sequentially pulled out of one crucible. Between two growth runs, the hot crucible is then refilled with silicon, which can be done in different ways [1]. The PVA Crystal Growing Systems GmbH has developed a mobile recharge system, which offers the unique possibility to serve several Cz-pullers time-delayed. To make the mobile feeding unit compact and easy to move, the hopper is separated from the passive conveyor, a quartz tube system. The connection of the hopper with the quartz tube is realized by a motor-driven active vibratory conveyor. As an advantage, the feeding rate can be predetermined and regulated, which in turn allows a high degree of automation of the feed process. Fig.8 shows the mobile recharge system in the process.

Figure 8: Mobile recharge system docked on Cz-puller

The interface from the feeder to the system is a special valve, which can be retrofitted to the special puller type. A more detailed description of the MRS system and the feed process can be found in [1].

One disadvantage of the multipulling technique may be the accumulation of impurities in the melt due to the segregation effect. An estimation of impurity accumulation in the melt due to the sequential melt replenishment has been published by Hopkins et al. [8].

The axial concentration profiles in Cz-ingots grown from replenished melts can be calculated as a function of the solidified fraction g, with C_0 is the initial concentration of the impurity in the liquid. The initial impurity concentration C_L^i (n) in the melt at the start of the n-th pull (3) can be calculated according to Hopkins with p = $(1\text{-}g)^{keff\text{-}1}$.

$$(3)\ C_L^i(n) = C_0\left[p^{n-1} + g\left(\frac{p^{n-1}-1}{p-1}\right)\right]$$

Fig. 9 shows the accumulation of impurities with a small segregation coefficient in the melt calculated for the sequential replenishment of the crucible. The refill is calculated after solidified fraction of 90% (g = 0.9).

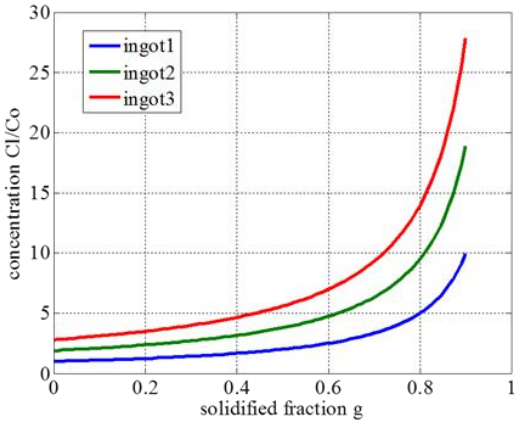

Figure 9: Impurity build-up curves for a replenished melt for the growth of 3 ingots in one crucible calculated according to Hopkins et al. [8].

For the calculation an effective distribution coefficient k_{eff} = 10^{-3} was applied, which is in the range for metal impurities, having a strong impact on the solar cell performance [9]. It can be estimated that the maximum accumulation of impurities in the melt with small segregation coefficients is less than a factor of 3.

2.4 Crystal growth and characterization

In our study, crystals were grown in different crystal growth configurations under the aspect of a high pull rate. All crystals were n-type with an axial distribution of the resistivity in the range of 4-1 Ωcm from top to tail. Tab.2 gives an overview of the studied crystal growth configurations and the main growth parameters. From the crystals labeled V1, V2, V5 grown in the configurations V1, V2 and V5 five slices were prepared equidistantly over the length of the ingots according to fig10. Additionally a longitudinal section was cut out for the investigation of the interface shape by means of LPS technique [10].

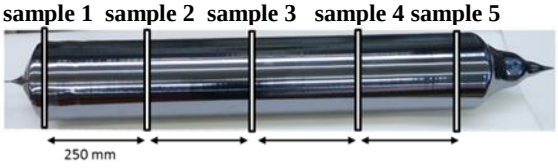

Figure 10: Position of the samples for characterization corresponding to a solidified fraction of g = 0.02 to 0.8.

The samples were subjected to FTIR measurements for the determination of interstitial oxygen and substituted carbon concentrations. The conversion factor is $3.14x10^{17}$ cm^{-2} for O_I and $1.0x10^{17}cm^{-2}$ for C_S. Measurements were taken 7 mm from the edge, half radius and in the center. The samples are designated 1 to 5 from top to tail. The results for the O_I-concentrations are summarized in tab.1. The C_S-concentration in 95% of all samples were below detection limit (<10^{16} cm^{-3}).

config. V1	sample 1	sample 2	sample 3	sample 4	sample 5	
center	10.8	9.1	8.2	7.5	6.5	x 10^{17} cm^{-3}
half radius	10.4	8.9	8.1	7.7	6.4	x 10^{17} cm^{-3}
edge	6.3	5.7	4.6	5.6	5.8	x 10^{17} cm^{-3}

config. V2	sample 1	sample 2	sample 3	sample 4	sample 5	
center	9.5	6.6	5.8	4.6	4.7	x 10^{17} cm^{-3}
half radius	9.2	6.6	5.6	4.0	4.3	x 10^{17} cm^{-3}
edge	3.6	3.2	2.3	1.6	3.6	x 10^{17} cm^{-3}

config. V5	sample 1	sample 2	sample 3	sample 4	sample 5	
center	9.8	6.9	6.7	7.8	9.3	x 10^{17} cm^{-3}
half radius	9.6	6.4	6.1	7.5	9.0	x 10^{17} cm^{-3}
edge	7.6	5.2	3.7	7.7	6.4	x 10^{17} cm^{-3}

Table 1: O_I-concentration in the crystals V1, V2, V5.

The measurement results do not have any statistical certainty. However, it can be concluded that the high pull speed in the configurations V2 and V5 does not have a negative effect on the distribution of oxygen and carbon content.

The minority carrier lifetime measurements on the crystal slices were measured with a Sinton BCT-400 / BLS-I (photoconductivity measurement) using the transient measuring method. The lifetime values were determined at a minority carrier density of 5 × 10^{14} cm^{-3}, which is usual for n-type material and are shown in figs. 11-13. The minority carrier lifetime is plotted versus the radial position on the different samples. The numbering of the samples (1 - 5) in tab.1 is replaced by the specification of the solidified fraction g (0.02 – 0.8).

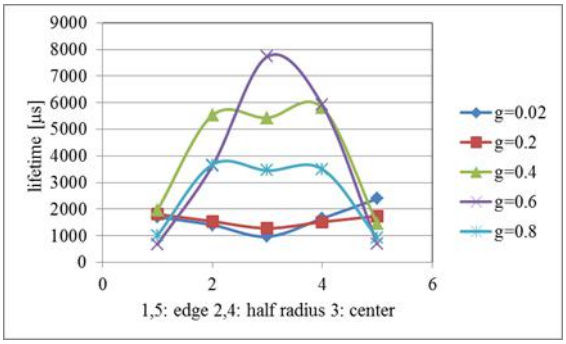

Figure 11: Minority carrier lifetime [µs] measured on the samples grown in crystal growth configuration V1

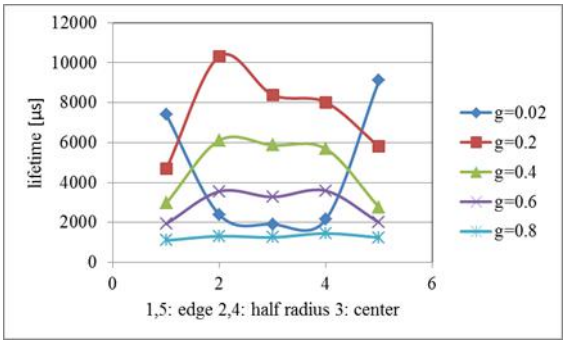

Figure 12: Minority carrier lifetime [µs] measured on the samples grown in crystal growth configuration V2

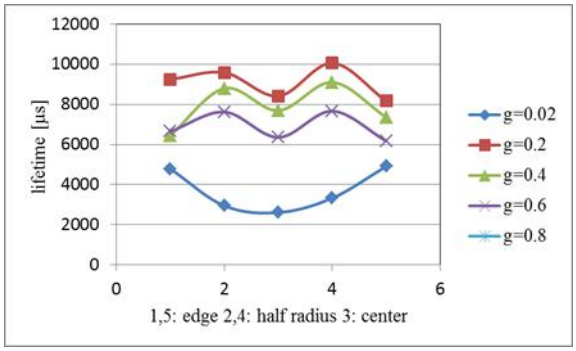

Figure 13: Minority carrier lifetime [µs] measured on the samples grown in crystal growth configuration V5. The sample 5 (g=0.8) was broken and could not be analyzed.

The distribution of the lifetime-reducing recombination centers should not be investigated or discussed in this context. However, it can also be stated here that the active crystal cooling in connection with the high pull speed does not appear to have a negative effect on the minority carrier lifetime distribution.

The phase boundary shape (concavity) was visualized on the longitudinal section using LPS technique at the Fraunhofer Center for Silicon Photovoltaics CSP. The results for the different crystal growth arrangements are shown in tab.2 and confirm the state diagram derived from the numerical simulation calculations in fig.3.

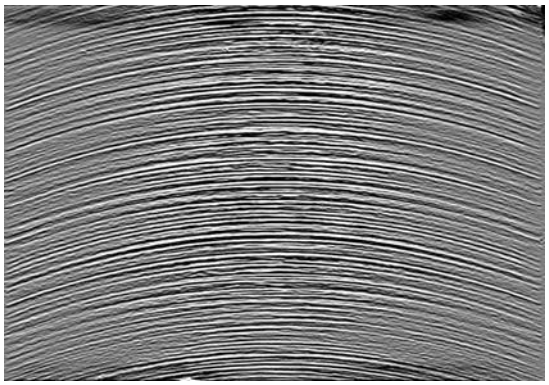

Figure 14: Growth striations revealed by the LPS technique [10] on a vertically sliced sample, indicating the deflection of the growth interface

growth configuration	hotzone	active crystal cooling	max. σ_{vM} [Mpa]	mean pull speed in body phase [mm/min]	measured deflection of interface in crystal center [mm]
V1	standard	no	$3.9*10^7$	0.9	13
V2	optimized	no	$4.6*10^7$	1.3	22
V3	optimized	standard	$4.8*10^7$	1.6	24
V4	optimized	optimized	$5.5*10^7$	1.7	21
V5	optimized	optimized	$6.5*10^7$	1.8	20

Table 2: Growth configurations with main parameters and calculated maximum occurring von Mises σ_{vM} stresses in the crystal at a length of 500 mm and the corresponding deflection of the interface.

Samples of ingots grown in crystal growth configuration V1, V2 and V5 were also evaluated by means of Scanning Infrared Stress Depolarization (SIRD). For this characterization technique we applied the SIRD system from PVA Metrology & Plasma Solutions GmbH. As silicon is optically isotropic in the unstressed state, residual stresses which may be present in the crystal due to the growth conditions lead to an optical anisotropy (stress birefringence), that can be evaluated with the SIRD system. A detailed description of this method can be found in [11]. Figs.15 -17 show three slices from the middle of the body of each examined crystal. For the characterization the samples were just etched. Therefore some saw marks can be seen.

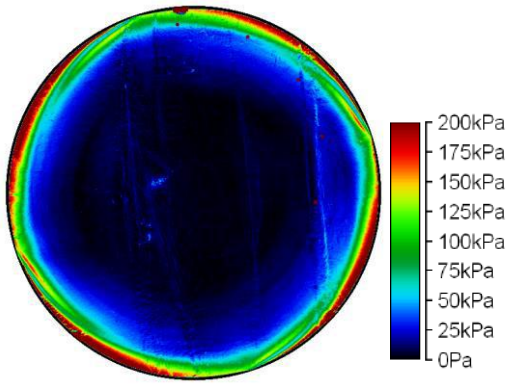

Figure 15: Shear stress maximum in the sample cut from the middle of a crystal grown in configuration V1

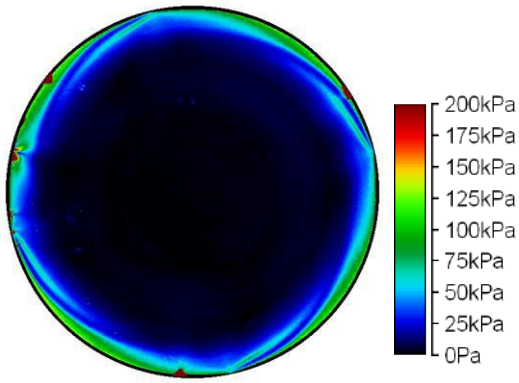

Figure 16: Shear stress maximum in the sample cut from the middle of a crystal grown in configuration V2

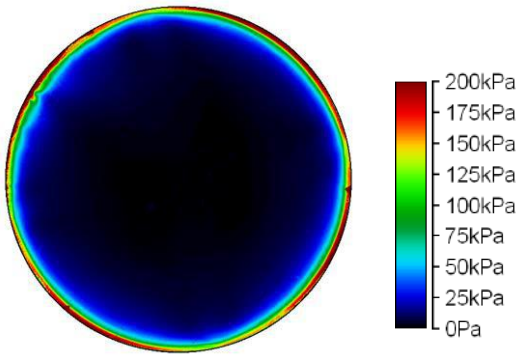

Figure 17: Shear stress maximum in the sample cut from the middle of a crystal grown in configuration V5

No differences between the examined samples were observed. All samples are stress-free except for the outer edge area. Along the circumference, the samples show slight tensile stresses, which may indicate a certain defect structure. A similar effect can also be observed in the lifetime distributions. Lifetimes measured on the as grown crystal surface show values lower than lifetimes measured 5 mm deep in the crystal volume. This effect was observed on several specially prepared crystals. An example is shown in fig.18.

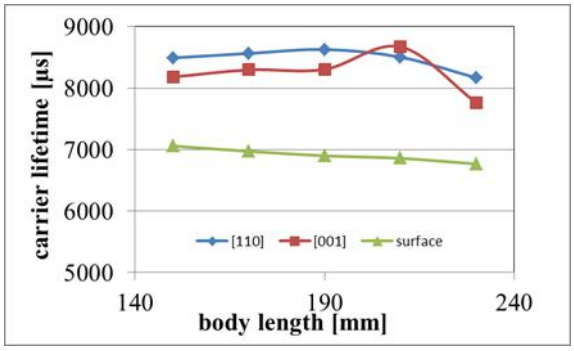

Figure 18: Minority carrier lifetime plotted versus a certain length in the body, measured on the as grown crystal and 5 mm beneath the surface

3 ECONOMIC ANALYSIS OF THE MULTIPULLING PROCESS COMBINED WITH ACTIVE CRYSTAL COOLING

An assessment of the economic potential cannot be presented quantitatively, because many factors depend on the technological condition of the process development as well as on the training level of the operational employees. Furthermore production costs may have different values depending on the location of the production plant and are subject to substantial fluctuations in the market. The cost savings of this growth technique is the reduced consumption of crucible material as well as the reduced amount of pot scrap (fig.21). The down-time of the multipulling process is less compared to a standard batch process. The biggest advantage is the drastic reduction of the process time and the resulting savings in process costs. This is shown in fig.19 where the power of the main heater and the bottom heater in a multipulling process of three ingots is compared with a standard batch process. The curves were derived from real crystal growth experiments performed at the crystal growth department of PVA CGS GmbH. The red curve represents a standard Cz-process with a pull speed of 0.9 mm/min in the body phase. The blue curve shows a multipulling process of three ingots grown with active crystal cooling and a mean pull speed of 1.8 mm/min in the body phase. Fig.20 shows a detailed section of Fig.19. The green line represents the individual crystal growth phases. Up to the first stage at about eight hours, the phases of pumping down, melting and stabilization of the melt take place. The steps represent the neck, shoulder, body and the end cone phase. After these steps the refilling phase takes place.

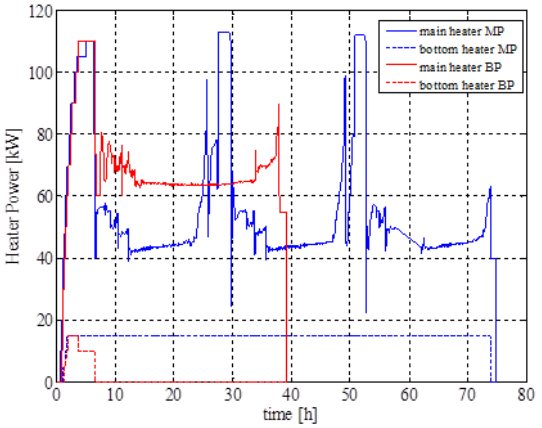

Figure 19: Power consumption of the main heater and the bottom heater versus process time for standard Cz (red curve) and multipulling process (blue curve).

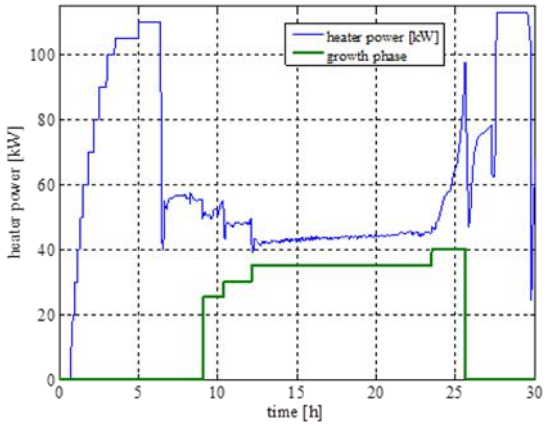

Figure 20: Detail of figure 19. The green line shows the different phases of a growth run (see text).

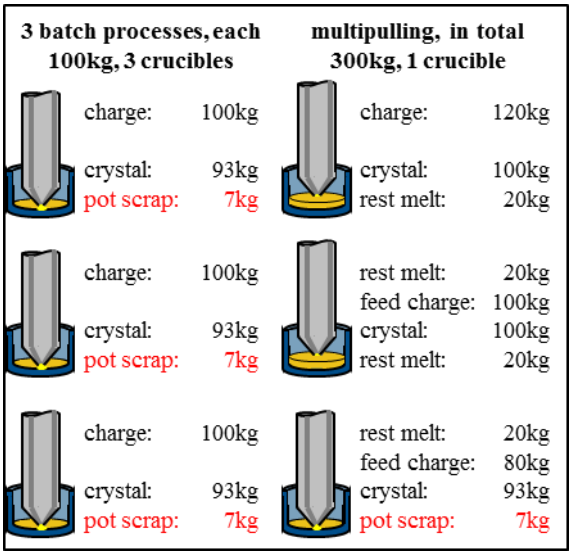

Figure 21: material consumption of a batch process compared to multipulling

Tab.3 shows the savings potential that results solely from the assumption of a higher pull rate. The main saving potentials are the process time and the reduced energy

consumption. The potential savings in columns 2 and 3 relate only to the body phase and are related to the standard process in configuration V1.

growth config.	mean pull speed [mm/min]	Δ time body phase [%]	Δ energy [%]
V1	0.9	0	0
V2	1.3	29	32
V5	1.8	49	53

Table 3: Time and energy savings of the different crystal growth configurations

4 CONCLUSIONS

The results presented in this paper demonstrate that the combination of multipulling and active crystal cooling has a tremendous cost reduction potential. In addition, these techniques still have an optimization potential, e. g. by the use of larger hot zones. This probably requires a new generation of Cz-pullers.

5 ACKNOWLEDGEMENTS

This work was supported by the German Ministry of Economy and Energy under contract number 0325883A.

6 REFERENCES

[1] F. Mosel, A.V. Denisov, B. Klipp, R. Sharma, R. Kunert, P. Dold, Proceedings 32nd European Photovoltaic Solar Energy Conference, München, Germany, (2016), 1064-1068
[2] CGSim package, STR Group,Ltd.
[3] F. Mosel, A.V. Denisov, B. Klipp, R. Kunert, P. Dold, Proceedings 33rd European Photovoltaic Solar Energy Conference, Amsterdam, Netherlands, (2017), 495-500
[4] E. Billig, Proc. Roy. Soc. (London) 229 (1955) 346-363
[5] V. Kalaev, A. Sattler, L. Kadinski, J. Crystal Growth 413 (2015) 12-16
[6] I. Drikis, M. Plate, J. Sennikovs, J. Virbulis, Journal of Crystal Growth (2016)
[7] W. von Ammon, E. Dornberger, P.O. Hansson, Journal of Crystal Growth **198/199** (1999) 390-398
[8] R.H. Hopkins et al., Journal of Crystal Growth **42** (1977), 493-498
[9] G. Coletti, Impurities in silicon and their impact on solar cell performance, thesis
[10] H.J. Schulze, A. Lüdge, H. Riemann, Electrochem. Soc. **143**, 4105 (1998)
[11] M. Herms, M. Wagner, Phys. Status Solidi C **12**, No.8, 1085-1089 (2015)